Am J Transl Res 2019;11(5):2843-2854
www.ajtr.org /ISSN:1943-8141/AJTR0089503

Original Article

Upregulation of the long noncoding RNA lncPolE contributes to intervertebral disc degeneration by negatively regulating DNA polymerase epsilon

Xingguo Li[1*], Zhenkai Lou[1*], Jie Liu[2], Hongkun Li[1], Yu Lei[1], Xueling Zhao[1], Fan Zhang[1]

[1]Department of Orthopedics, The First Affiliated Hospital of Kunming Medical University, Kunming 650032, Yunnan, China; [2]Department of Orthopedics, The First People's Hospital of Yunnan, Kunming 650032, Yunnan, China. [*]Equal contributors.

Received December 6, 2018; Accepted March 8, 2019; Epub May 15, 2019; Published May 30, 2019

Abstract: Long noncoding RNAs (lncRNAs) are critical regulators of gene transcription. Our previous results have demonstrated that iron deficiency accelerates intervertebral disc degeneration (IDD) by affecting the stability of the DNA polymerase epsilon (Polε) complex. Here, we discovered that the novel lncRNA lncPolE functions as a negative regulator of Polε. The expression of lncPolE in IDD tissues was upregulated compared to its expression in healthy control tissues, and this was in contrast to the PolE1 expression levels. The increased lncPolE level was significantly correlated with the severity of IDD. Ectopic expression of lncPolE in human nucleus pulposus cells (hNPCs) was able to decrease *PolE1* levels and cause apoptosis, while the specific knockdown of lncPolE in primary NP cells (pNPCs) from IDD patients can restore *PolE1* levels. Interestingly, iron depletion or supplementation can affect the expression of lncPolE. Further analyses indicated that the downregulation of DNA methylation in the promoter region of lncPolE caused its overexpression. Collectively, our results suggest that the aberrant expression of lncPolE contributes to the pathogenesis of IDD by negatively regulating *PolE1* in iron deficient conditions, and this may provide a new avenue to alleviate IDD progression in clinical treatment.

Keywords: IDD, lncRNA, PolE, lncPolE, apoptosis, iron deficiency

Introduction

The vast majority of people encounter low back pain (LBP) with age, which causes severe economic and social burdens [1, 2]. Intervertebral disc degeneration (IDD), a multifactorial disease caused by genetic and environmental factors (e.g., inflammation and apoptosis), is known as a significant cause of LBP [3, 4]. Intervertebral discs (IVDs) consist of the following three parts: cartilage endplates, annulus fibrosus (AF) and nucleus pulposus (NP) from the outside to the inside of the disc [5, 6]. The outer endplates serve as the interface between rigid vertebral bodies and pliant intervertebral disks, and they can absorb the small molecules and nutrients required for NP and AF cells [5, 6]. The middle AF is the tough circular exterior of the IVD that surrounds the soft inner NP [5, 6]. Human clinical trial and animal model studies have documented that many signaling pathways are involved in the process of IDD. For instance, the Notch pathway is activated by hypoxia in AF cells [7], and the treatment of tumor necrosis factor alpha (TNF-α) or interleukin 1 beta (IL-1β) in NP cells can induce the expression of Notch-1 and Notch-2, two Notch receptors [8, 9]. The transcription factor nuclear factor kappa β (NF-κB) and mitogen-activated protein kinase (MAPK) pathways can mediate the inflammation process by regulating proinflammatory mediators, such as TNF-α, IL-1β, and IL-6 [10, 11]. The apoptotic pathway is also involved in IDD by regulating the levels of Bcl-2, caspase-3, collagen and aggrecan (ACAN) in NP cells [12-14].

Emerging studies have demonstrated that long noncoding RNAs (lncRNAs), an important class of the noncoding RNA family that are longer than 200 nt, play critical roles in the pathogenesis of many diseases (e.g., cancers, cardiovas-

cular disease and neurodegenerative disorders) by affecting diverse biological processes, such as cell differentiation, cell cycle progression and apoptosis [15-18]. Recently, a few studies have also focused on revealing lncRNA profiles in the process of IDD [19, 20]. Some of them have demonstrated how these lncRNAs contribute to IDD [19-22]. For instance, Linc-ADAMTS5, a long intergenic noncoding RNA, cooperates with Ras-responsive element-binding protein 1 (RREB1) to contribute to IDD pathogenesis by inhibiting the expression of *ADAMTS5* (a disintegrin and metalloproteinase with thrombospondin motif-5) in NP cells [21]. The lncRNA *NEAT1* plays a role in the occurrence and development of IDD by regulating the levels of *MMP13* (matrix metallopeptidase 13) and *ADAMTS5*, as well as affecting the extracellular-signal-regulated kinase (ERK)/MAPK signaling pathway in degenerative NP cells [22]. These findings revealed the significance of studying the roles of IDD-associated lncRNAs, which may enhance our understanding of the molecular basis of IDD initiation and progression. In addition, current evidence has indicated that aberrant histone acetylation or DNA methylation in the promoter region of lncRNAs can result in the differential expression of lncRNAs [23-25].

Our most recent study showed that iron deficiency causes the downregulation of DNA polymerase epsilon (Polε), which activates apoptotic pathways and eventually leads to the occurrence of IDD [26]. The mammalian Polε complex is composed of the four following subunits: PolE1 (catalytic subunit), PolE2, PolE3, and PolE4 [26, 27]. Our results have shown that *PolE1* is regulated at the transcriptional level under low iron conditions [27]. Thus, we next sought to determine whether lncRNAs were involved in the regulation of this process. For this purpose, we performed a lncRNA-specific microarray and found that lncPolE can negatively regulate the expression of *PolE1*. Here, we revealed the role of lncPolE in the regulation of *PolE1* expression, and we also investigated the underlying mechanism of lncPolE upregulation in IDD patients.

Materials and methods

Clinical samples from IDD patients

The blood samples were collected from 24 healthy volunteers and 120 IDD patients who underwent surgery and therapy from 2014 to 2016 at the Department of Orthopedics at the First Affiliated Hospital of Kunming Medical University, Kunming, Yunnan, China. These 120 IDD patients were divided into five groups according to their Pfirrmann grades (from 1 to 5, n=24 in each group). In addition, degenerative tissue samples from five IDD patients (one sample from each Pfirrmann grade) were collected. All of these samples were collected according to protocols that were approved by the ethical board of Kunming Medical University. The basic information (average age and their Pfirrmann grades) of the IDD patients is shown in Table S1.

Cell culture and transfection

Human NP cells (hNPCs) were obtained from ScienCell Research Laboratories (Cat. #4800) and were grown with the previous method [26]. Cell transfection was performed as previously described [26]. Briefly, lncPolE-specific siRNA (TGTGGGTTCCAGTGTGTCCTGTGAT) or pCDNA3-lncPolE was transfected into hNPCs using Lipofectamine 2000 (Invitrogen, USA, Cat. #116-68027). After incubation at 37°C for 48 hr, the transfected cells were used in the required experiments.

Isolation of the primary nucleus pulposus cells (pNPCs)

The primary pNPCs were isolated as described previously [28]. Briefly, the separated NP tissues were washed with Dulbecco's Modified Eagle Medium (DMEM) (Thermo Fisher Scientific, USA, Cat. #11965-084) supplemented with 100 μg/mL kanamycin (Thermo Fisher Scientific, Cat. #11815-024) and 100 μg/mL gentamycin (Thermo Fisher Scientific, Cat. #15750-078). The tissues were then cut into 1-2 mm pieces, followed by an incubation in DMEM/F12 medium (Thermo Fisher Scientific, Cat. #10565042) supplemented with 10% fetal bovine serum (FBS) (Thermo Fisher Scientific, Cat. #10437028) in a 25-cm^2 flask. The culture medium was changed twice per week. After 3-4 weeks, the attached cells were collected and subjected to the required experiments.

RNA isolation and quantitative RT-PCR (qRT-PCR) analysis

The total RNA from the tissues and cultured cells was extracted using the TRIzol™ kit (Th-

ermo Fisher Scientific, Cat. #15596026). The first-strand cDNA of each sample was generated using a High-Capacity cDNA Reverse Transcription Kit (Thermo Fisher Scientific, Cat. #4368814) following the manufacturer's instructions. After a dilution of 10-fold, the cDNA was subjected to qRT-PCR analysis with the previously used primers. The $2^{-\Delta\Delta Ct}$ method was used to determine the fold change of individual gene expression.

Microarray analysis

The microarray analysis was carried out as described previously [29]. Briefly, 0.5 μg total RNA from one healthy control and from five IDD patients with different Pfirrmann grades (from 1 to 5, one patient per grade) was used to synthesize cDNA using a GeneChip 3' *In Vitro* Transcription (IVT) Express Kit (Thermo Fisher Scientific, Cat. #902789). Following this, the cDNA was fragmented and hybridized with a Human LncRNA Expression Array V4.0 (Arraystar Inc. USA, Cat. #AS-LNC-H-V4.0), which contained 40,173 human lncRNA probes. After hybridization, the chip was washed and scanned with a GeneChip™ Scanner 3000 7G system (Thermo Fisher Scientific, Cat. #000213).

Western blot analysis

The protein levels were determined by western blotting as described previously [30]. Briefly, equal amounts of cell lysates were subjected to electrophoresis, followed by transferring the proteins to a nitrocellulose membrane (Thermo Fisher Scientific, Cat. #LC2009) and probing them with the primary antibodies as described previously [30]. After incubation with peroxidase-labeled secondary antibodies, the enhanced chemiluminescence (ECL) signals were recorded using a ChemiDoc MP (Bio-Rad, USA, Cat. #17001402).

Flow cytometry analysis

Flow cytometry assays were performed as described previously [26]. In brief, a total of 10^4 cells that were grown in culture dishes were resuspended in 100 μL of binding buffer. Then, the cells were stained with a PE Annexin V Apoptosis Detection Kit (BD Biosciences, USA, Cat. #559763). After an incubation at 23°C for 20 min, the cells were used for flow cytometry assays with a FACScan machine (BD Biosciences, USA).

Quantitative methylation-specific PCR (qMSP)

The qMSP was performed as described previously [31]. Briefly, the genomic DNA was isolated with a Genomic DNA Purification Kit (Thermo Fisher Scientific, Cat. #K182104A) according to the manufacturer's methods. For each sample, 0.8 μg of genomic DNA was treated with sodium bisulfite using the EZ DNA Methylation-GOLD Kit (ZYMO Research, USA, Cat. #D5008) following the manufacturer's instructions. The resulting genomic DNA was subjected to PCR analysis with the primers listed in Table S2.

Statistical analysis

All experiments in the current study were repeated three times independently. The statistical analyses of the experimental data were performed using a two-tailed Student's *t*-test. The significance was set at $P < 0.05$, and the data are represented as the mean ± standard deviation (SD).

Results

Identification of differentially expressed lncRNA profiles in IDD patients

Our previous results have shown that PolE1 and its interacting proteins, including PolE2, -3 and -4, were markedly decreased in severe IDD patients [26]. To identify if lncRNAs are involved in the regulation of these *PolE*s, we randomly selected one degenerative sample from each Pfirrmann grade (1-5) and used one nondegenerative IVD tissue from a patient who had been in a car accident and needed surgery to repair his IVD as a control. After RNA extraction, we subjected these 6 samples to a microarray analysis. Out of a collection of 40,173 lncRNA probes, we found that the expression of a total of 146 lncRNAs was consistently increased or decreased in different IDD patients. Of those, 61 lncRNAs were upregulated, while the other 85 lncRNAs were downregulated (Table S3). As shown in the heat map, we indicated the top 15 upregulated and top 15 downregulated lncRNAs (**Figure 1A**). In the upregulated group, ENST00000544414.1 showed the greatest increase (nearly 33.5-fold) in the Pfirrmann grade 5 patient. In the downregulated group, ENST00000415358.1 demonstrated the greatest decrease (nearly 55.4-fold) in the Pfirrmann grade 5 patient. To verify the accuracy of the

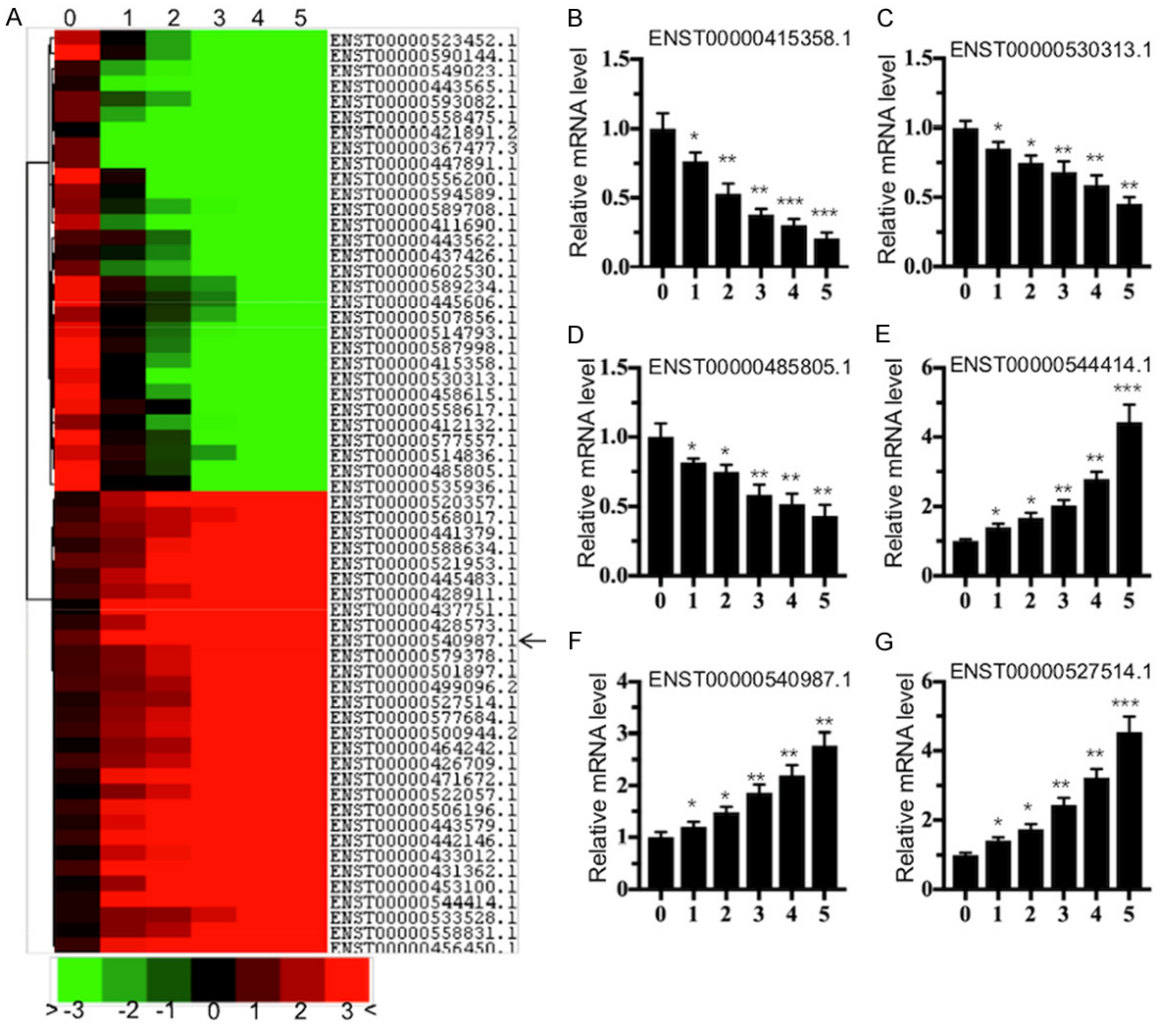

Figure 1. The aberrantly expressed lncRNA profile in IDD patients. (A) The heat map of the top 15 downregulated and top 15 upregulated lncRNAs in IDD patients. The total RNA from a healthy control (0) and from five IDD patients with different Pfirrmann grades (from 1 to 5, one sample per grade) was subjected to a microarray analysis. The heat map indicated high (red) or low (green) levels of lncRNA expression. (B-G) The verification of lncRNA levels in IDD patients. qRT-PCR was performed to verify the expression of three downregulated lncRNAs, including ENST00000415358.1 (B), ENST00000530313.1 (C), and ENST00000485805.1 (D), and three upregulated lncRNAs, including *ENST00000544414.1* (E), ENST00000540987.1 (F), and ENST00000527514.1 (G). **P* < 0.05, ***P* < 0.01, and ****P* < 0.001.

microarray results, we selected 6 lncRNAs to quantify their expression by qRT-PCR using the same RNA samples in the microarray analysis. Of these lncRNAs, three, including ENST00000415358.1, ENST00000530313.1 and ENST00000485805.1, were from the downregulated group, and the other three, including ENST00000544414.1, ENST00000540987.1 and ENST00000527514.1, were from the upregulated group. Consistent with the microarray results, the expression levels of ENST00000415358.1, ENST00000530313.1 and ENST00000485805.1 gradually decreased with the increasing severity of IDD patients (**Figure 1B-D**), whereas the levels of ENST00000544414.1, ENST00000540987.1 and ENST00000527514.1 were reversed (**Figure 1E-G**).

LncPolE is upregulated in IDD patients

Given that many lncRNAs are antisense and that they have been reported to act on gene expression in multiple model organisms, one sample way to determine whether these differentially expressed lncRNAs can regulate *PolE* expression is to map their chromosome loca-

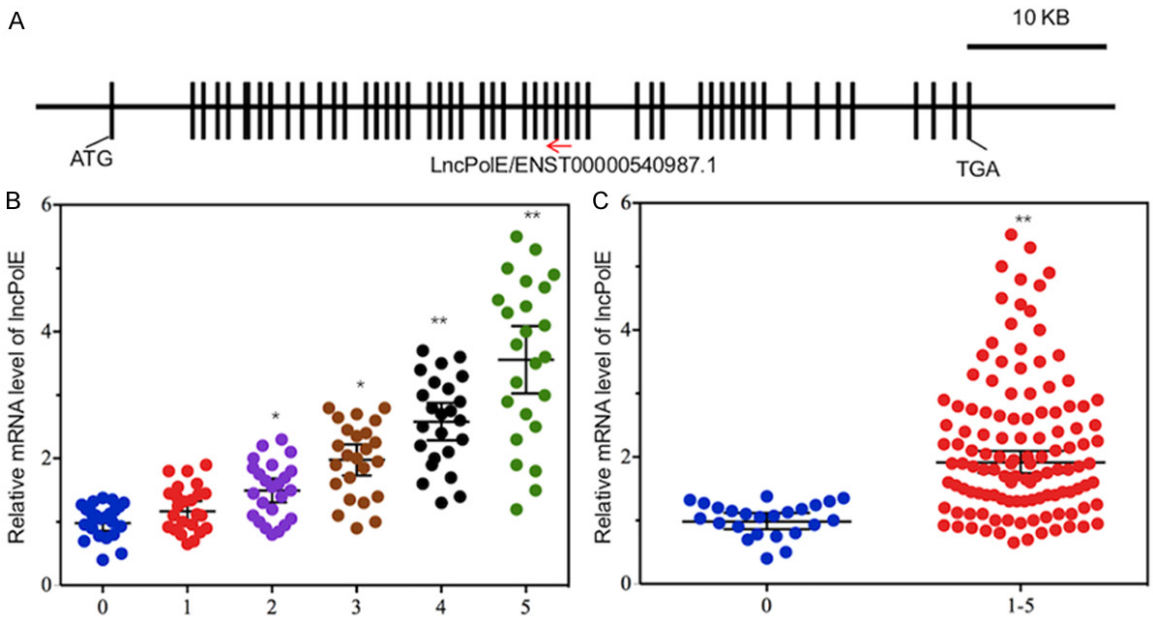

Figure 2. lncPolE expression was increased in IDD patients. A. A schematic diagram of the *PolE1* gene and the location of lncPolE. The exons of the *PolE1* gene are shown as black boxes, and lncPolE is located across the 28th and 29th exons. B and C. The expression of lncPolE was elevated in IDD patients. Venous blood samples were collected from healthy controls (n=24) and 120 IDD patients with different Pfirrmann grades (from 1 to 5, n=24 patients in each grade). The RNA from these samples was subjected to an analysis of lncPolE levels. $*P < 0.05$, $**P < 0.01$.

tions. After carefully comparing their chromosome positions, we found that ENST00000540987.1 was located across the 28th and 29th exons of *PolE1* (**Figure 2A**), and its direction was opposite to that of the *PolE1* gene. Given that ENST00000540987.1 was upregulated and *PolE1* was downregulated in IDD tissues, we speculated that ENST00000540987.1 was an antisense lncRNA of *PolE1* and that it might negatively affect *PolE1* levels. To further investigate its role and to simplify its name, we termed ENST00000540987.1 as lncPolE in the following study. Our previous results have shown that the *PolE1* level was negatively associated with the severity of disc degeneration. To investigate whether the expression level of lncPolE was correlated with disc degeneration, we measured its level in different Pfirrmann grade patients. As shown in **Figure 2B**, our results indicated that the lncPolE level was positively associated with the severity of Pfirrmann grades, that is, the higher grades, the higher the lncPolE level. In addition, we also combined all of the relative expression levels of lncPolE in IDD patients and then compared them with those in the healthy controls. Similarly, we also observed a significant increase in lncPolE in IDD patients (**Figure 2C**).

Overexpression of lncPolE results in the repression of PolEs and leads to apoptosis

To investigate whether lncPolE can regulate *PolE1* expression, we constructed a pCDNA3-lncPolE vector and transfected it into NP cells, followed by measuring the expression levels of lncPolE and *PolE1*. As shown in **Figure 3A** and **3B**, the overexpression of lncPolE resulted in the repression of *PolE1*. Given that our previous results have shown that the downregulation of *PolE1* in NP cells caused the instability of the PolE complex and led to apoptosis, we next sought to evaluate the effect of lncPolE overexpression on the stability of the PolE complex and the apoptotic status of cells. Our results indicated that the overexpression of lncPolE not only resulted in a decrease in the PolE1, -2 and -3 protein levels but also induced apoptosis because of the activation of caspase-3, -9, and PARP (poly (ADP-ribose) polymerase 1) (**Figure 3C**). In addition, we also stained the lncPolE overexpression cells with Annexin V-PE and 7-AAD and detected the cellular apoptosis status with flow cytometry. The results showed that lncPolE overexpression significantly increased the cell population in Q2 (early apoptosis) and Q3 (late apoptosis) com-

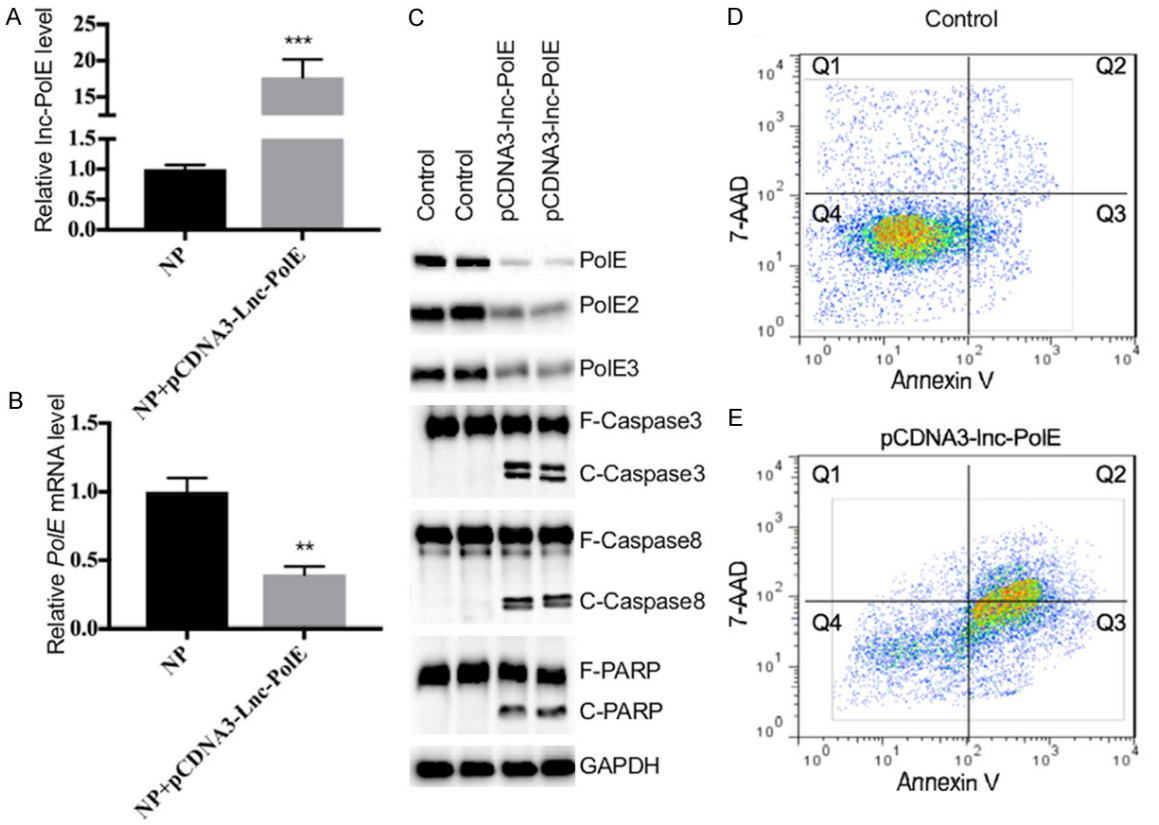

Figure 3. The *in vitro* overexpression of lncPolE inhibited *PolE1* expression and induced apoptosis. Human NP cells (hNPCs) were infected with a pCDNA3 empty vector (control) and pCDNA3-lncPolE. After incubation for 48 hr, the cells were subjected to an analysis of the lncPolE levels (A) and the *PolE1* mRNA levels (B), as well as an analysis of the protein levels of PolE1, PolE2, PolE3, Caspase-3, Caspase-8 and PARP. GAPDH was used as a loading control (C). (D and E) The same cells used in (A) were stained with Annexin V-PE/7-AAD and were subjected to flow cytometry analysis. (D) Control cells and (E) cells transfected with pCDNA3-lncPolE.

pared to the population of the control cells (**Figure 3D** and **3E**), which suggests that lncPolE overexpression was able to induce apoptosis.

Knockdown of lncPolE in NP cells increases PolE levels and reverses apoptosis

Our above results indicated that the increase of lncPolE resulted in the instability of the PolE complex and induced apoptosis. To further evaluate whether the upregulation of lncPolE is the fundamental cause of this phenomenon, we next attempted to knockdown lncPolE in pNPCs from IDD patients and then detect the PolE complex levels and apoptotic proteins. Accordingly, we isolated pNPCs from a healthy tissue and two IDD tissues with Pfirrmann grades 2 and 4. After transfection with lncPolE-specific siRNA for 48 hr, we measured the mRNA levels of lncPolE and *PolE1*, as well as the protein levels of the PolE complex and apoptotic proteins, including caspase-3, -9, and PARP. As expected, we significantly knocked down the lncPolE levels in pNPCs from IDD tissues (**Figure 4A**), which resulted in a dramatic increase in the *PolE1* mRNA levels (**Figure 4B**) and caused the accumulation of the PolE complex (**Figure 4C**). Meanwhile, the knockdown of lncPolE in primary NP cells also led to the inhibition of apoptosis compared to that in nontransfected cells because of the inactivation of caspase-3, -9, and PARP (**Figure 4C**).

Iron depletion or supplementation changes the lncPolE levels

Our previous results showed that iron supplementation with $FeCl_3$ in pNPCs from IDD tissues increased the protein levels of PolE1, -2 and -3 but decreased the levels of apoptotic proteins [26]. In contrast, iron depletion with the chelator deferoxamine (DFO) in hNPCs ca-

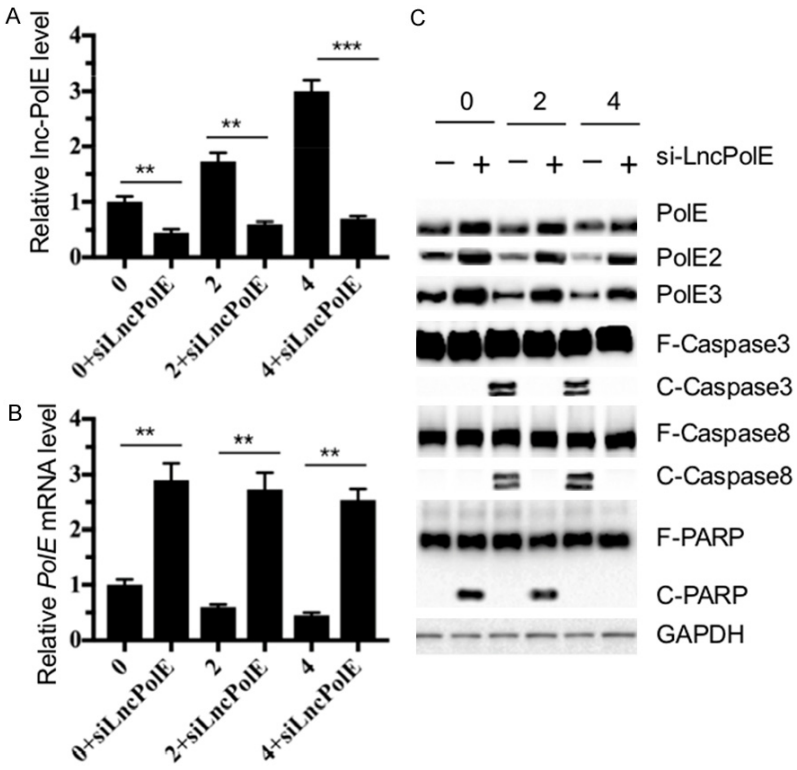

Figure 4. The *in vitro* knockdown of lncPoIE resulted in the increase of *PoIE1* expression and inhibited apoptosis. The primary NP cells (pNPCs) that were isolated from one healthy control (0) and from two IDD patients with the Pfirrmann grades 2 and 4 were transfected with lncPoIE-specific siRNA. The resulting cells were incubated for another 48 hr and were then used to measure the lncPoIE levels (A), *PoIE1* mRNA levels (B), and protein levels of PoIE1, PoIE2, PoIE3, Caspase-3, Caspase-8 and PARP. GAPDH was used as a loading control (C).

used a decrease in PoIE1, -2 and -3 but an induction of apoptotic proteins. To further determine whether iron depletion or supplementation can affect the lncPoIE levels, we primarily treated hNPCs with different concentrations of DFO (0, 20, 40 and 60 μM), followed by the detection of the mRNA levels of lncPoIE and *PoIE1*. As shown in **Figure 5A**, the lncPoIE levels gradually increased with increasing DFO concentrations. However, the mRNA level of *PoIE1* gradually decreased with increasing DFO concentrations (**Figure 5B**). In addition, we also treated pNPCs that were isolated from one healthy control and two IDD tissues with different Pfirrmann grades (2 and 4) using 100 μM $FeCl_3$. After 24 hr of incubation, we observed that iron supplementation resulted in a dramatic decrease in the lncPoIE level in two degenerative cells compared to that in their corresponding untreated cells (**Figure 5C**). In contrast, iron supplementation led to a significant increase in the *PoIE1* mRNA levels in these two degenerative cells (**Figure 5D**). We did not observe significant changes in either of the lncPoIE and *PoIE1* levels in healthy NP cells under conditions with or without $FeCl_3$ treatment (**Figure 5C** and **5D**).

The decreased DNA methylation level in the promoter of lncPoIE causes the upregulation of lncPoIE

Our above results verified the increase in lncPoIE levels in IDD tissues and in hNPCs treated with DFO. Thus, we next sought to investigate the underlying mechanism of its upregulation. Currently, dysregulated DNA methylation and acetylation in the promoters of lncRNAs are the two primary mechanisms that cause the differential expression of lncRNAs. Based on this notion, we primarily analyzed the promoter sequence of lncPoIE and found two CpG islands located in the regions of (-)430-(-)357 and (-)932-(-)823 (**Figure 6A**). Because DNA methylation often occurs at CpG islands, we speculated that disrupted DNA methylation in the promoter of lncPoIE might be the primary reason for its overexpression in IDD tissues. To verify this hypothesis, we examined the DNA methylation level of CpG islands in healthy and degenerative NP cells with the qMSP method. As shown in **Figure 6B**, our results indicate that the methylation levels of both CpG islands were dramatically decreased in degenerative NP cells compared to healthy pNPCs. To further verify that the DNA methylation level affects lncPoIE expression, we treated hNPCs with the DNA methylation inhibitor 5-aza-2'-deoxycytidine (AZA, 1 μM) and with the acetylation inhibitor trichostatin A (TSA, 300 nM) in combination with or without DFO (30 and 60 μM), followed by measuring the DNA methylation levels of CpG islands and the lncPoIE level. Our results indicated that in comparison to the methylation levels with DMSO treatment, the methylation

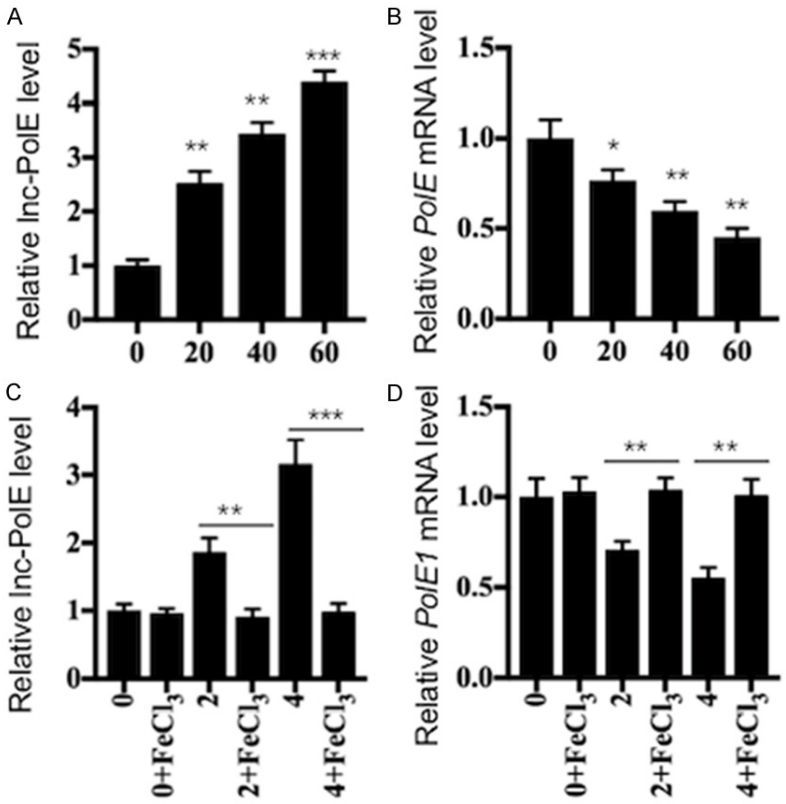

Figure 5. Iron depletion and supplementation affected the lncPolE and *PolE1* levels. The hNPCs were treated with different concentrations (0, 20, 40 and 60 μM) of DFO for 24 hr. The cells were then harvested and subjected to an examination of their lncPolE levels (A) and *PolE1* mRNA levels (B). $*P < 0.05$, $**P < 0.01$, and $***P < 0.001$. The pNPCs from healthy controls (0) and from two IDD patients with Pfirrmann grades 2 and 4 were treated with or without 100 μM $FeCl_3$ for 24 hr. Following this, the cells were harvested and subjected to an examination of their lncPolE levels (C) and *PolE1* mRNA levels (D). $**P < 0.01$, and $***P < 0.001$.

levels of both CpG islands were markedly decreased with AZA treatment but not with TSA treatment (**Figure 6C** and **6D**). In contrast, the expression level of lncPolE was significantly increased in the AZA treatment compared to the level in the DMSO or TSA treatments (**Figure 6E**). In addition, we also found that the treatments of DFO in combination with DMSO or TSA dramatically decreased the methylation levels of both CpG islands (**Figure 6C** and **6D**) but significantly increased the lncPolE levels (**Figure 6E**). However, we did not observe significant changes in DNA methylation or lncPolE levels when cells were treated with DFO and AZA (**Figure 6C-E**). At the same time, we also measured the *PolE1* mRNA levels in these treatments, and the results showed that AZA treatment, but not TSA treatment, caused its downregulation (**Figure 6F**). These results clearly indicated that dysregulated DNA methylation in the promoters of lncPolE played a significant role in the regulation of *PolE1* levels.

Discussion

Iron deficiency is a critical cause of many diseases because iron is an essential cofactor for proteins [32, 33]. Our recent study has revealed that iron deficiency results in the instability of the DNA polymerase epsilon complex, which leads to cell apoptosis and the pathogenesis of IDD [26]. In the present study, we further investigated the underlying mechanism regarding PolE1 downregulation in IDD tissues. Our results suggest that cells need to maintain a certain DNA methylation status to regulate noncoding RNA and gene expression under normal conditions. The DNA methylation status determines the lncPolE level, which negatively regulates *PolE* expression (**Figure 7**). In degenerative cells from IDD tissues, the DNA methylation level dramatically decreased in the promoter of lncPolE, which caused the upregulation of lncPolE. The elevated level of lncPolE represses PolE1 expression, which affects the stability of the PolE complex and induces apoptosis, eventually leading to the pathogenesis of IDD (**Figure 7**).

In recent years, noncoding RNAs, in particular, microRNAs (miRNAs), and lncRNAs have been identified to be widely involved in the pathogenesis of IDD [34-37]. In the present study, we found a total of 146 differentially expressed lncRNAs in IDD tissues. Importantly, these lncRNAs were not only differentially expressed in IDD tissues, but their expression levels also seemed to be associated with the severity of disc degeneration. These results suggest that they are IDD-dependent lncRNAs. Although we do not examine how these lncRNAs (except for

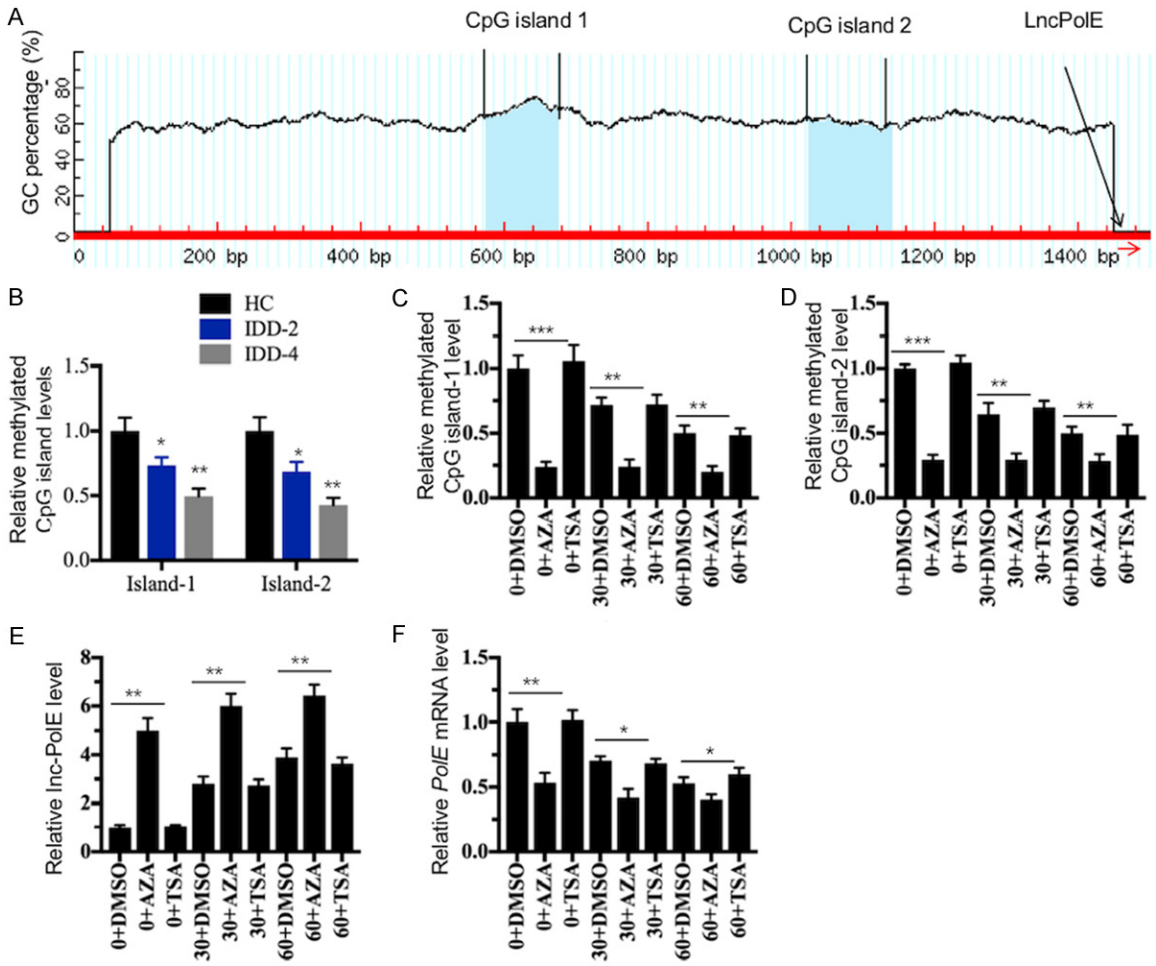

Figure 6. Dysregulated DNA methylation levels contributed to lncPolE overexpression in IDD tissues. (A) A schematic diagram of the CpG islands in the promoter of lncPolE. The promoter of lncPolE (1500 bp length) had two CpG islands (1 and 2). The position of lncPolE is indicated by a red arrow. (B) The methylation levels of two CpG islands were significantly downregulated in IDD tissues. qMSP was performed to examine the DNA methylation levels of both CpG islands in one healthy control (HC) and in two IDD tissues with Pfirrmann grades 2 and 4 (IDD-2 and -4, respectively). $*P < 0.05$, and $**P < 0.01$. (C and D) AZA treatment significantly downregulated the DNA methylation levels of both CpG islands. The hNPCs were treated with DMSO, 1 μM of AZA or 300 nM of TSA in combination with different concentrations of DFO (0, 30 and 60 μM). The qMSP was then performed to examine the DNA methylation levels of both CpG islands. $**P < 0.01$, and $***P < 0.001$. (E and F) AZA treatment significantly upregulated the lncPolE levels but downregulated *PolE1* expression. The cells used in B were subjected to an examination of their lncPolE levels (E) and PolE1 expression levels (F), respectively. $*P < 0.05$, and $**P < 0.01$.

lncPolE) function in the process of IDD, we speculate that our microarray data provide evidence for future studies in the field of lncRNAs and their involvement in IDD pathogenesis. In our recently published work, we performed a microarray to identify genes that are differentially expressed in IDD tissues, and we identified a total of 327 differentially expressed genes. A critical future work is to analyze these two microarray results and to determine whether the dysregulated lncRNAs can regulate those differentially expressed genes.

Through the *in vitro* knockdown and overexpression experiments, we verified that *PolE1* was negatively regulated by lncPolE. We also found that dysregulated DNA methylation levels are the basic cause of lncPolE overexpression in IDD tissues. Given that DNA methylation occurs by the addition of a methyl (CH3) group to DNA with DNA methyltransferases (DNMTs) [38, 39], we will determine the DNMT levels in IDD tissues and investigate whether DNMTs are involved in the regulation of lncPolE levels. One interesting phenomenon observed in this

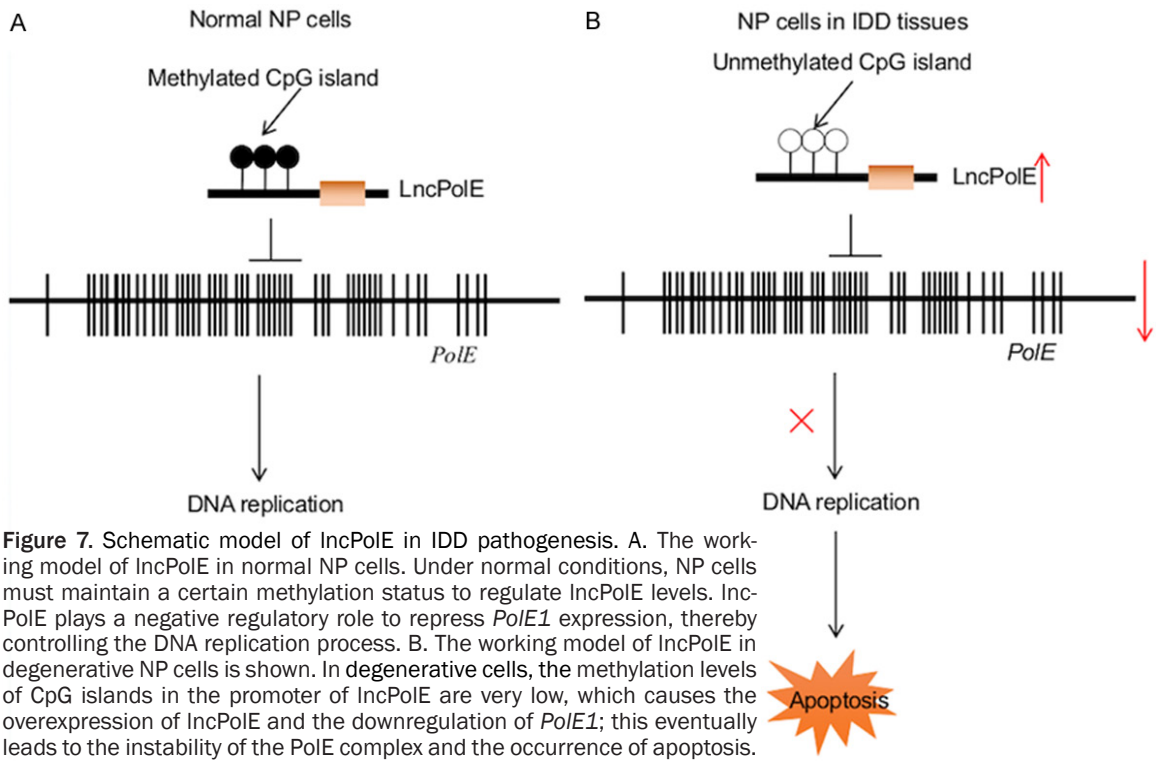

Figure 7. Schematic model of lncPoIE in IDD pathogenesis. A. The working model of lncPoIE in normal NP cells. Under normal conditions, NP cells must maintain a certain methylation status to regulate lncPoIE levels. lncPoIE plays a negative regulatory role to repress *PoIE1* expression, thereby controlling the DNA replication process. B. The working model of lncPoIE in degenerative NP cells is shown. In degenerative cells, the methylation levels of CpG islands in the promoter of lncPoIE are very low, which causes the overexpression of lncPoIE and the downregulation of *PoIE1*; this eventually leads to the instability of the PoIE complex and the occurrence of apoptosis.

study is that the intracellular iron levels were able to regulate the lncPoIE levels. By the supplementation of iron in pNPCs from IDD tissues, we observed a significant decrease in the lncPoIE levels (**Figure 5C**). However, iron depletion in hNPCs causes an increase in the lncPoIE levels (**Figure 5A**). To our knowledge, this is the first lncRNA that can be regulated by a metal ion. However, we do not know whether it is directly regulated by the metal ion. One possibility is that iron regulates the *PoIE1* level, which in turn, has a feedback effect on lncPoIE. Several assays, including the knockdown of DMT1 (iron divalent metal transporter 1) or TfR1 (iron transferrin receptor 1), can be performed to verify this possibility.

Conclusion

In this study, we identified the new lncRNA lncPoIE that can negatively regulate *PoIE1* expression. The decreased DNA methylation level in the promoter of lncPoIE causes its overexpression and leads to *PoIE1* downregulation in degenerative cells. The instability of the PoIE complex induces apoptosis and results in the pathogenesis of IDD.

Acknowledgements

This study was supported by a grant from the National Natural Science Foundation of China (No. 81601939) and two grants from Yunnan Applied Basic Research Projects (No. 2017FE-468-145 and No. 2018FB125).

Disclosure of conflict of interest

None.

Address correspondence to: Jie Liu, Department of Orthopedics, The First People's Hospital of Yunnan, Kunming 650032, Yunnan, China. E-mail: pacemakerliu@126.com; Fan Zhang, Department of Orthopedics, The First Affiliated Hospital of Kunming Medical University, Kunming 650032, Yunnan, China. E-mail: zhangfan@kmmu.edu.cn

References

[1] Wong AY, Karppinen J, Samartzis D. Low back pain in older adults: risk factors, management options and future directions. Scoliosis Spinal Disord 2017; 12: 14.

[2] Awosan KJ, Yikawe SS, Oche OM, Oboirien M. Prevalence, perception and correlates of low back pain among healthcare workers in tertiary health institutions in Sokoto, Nigeria. Ghana Med J 2017; 51: 164-174.

[3] Feng Y, Egan B, Wang J. Genetic factors in intervertebral disc degeneration. Genes Dis 2016; 3: 178-185.

[4] Martirosyan NL, Patel AA, Carotenuto A, Kalani MY, Belykh E, Walker CT, Preul MC, Theodore

N. Genetic alterations in intervertebral disc disease. Front Surg 2016; 3: 59.
[5] Pattappa G, Li Z, Peroglio M, Wismer N, Alini M, Grad S. Diversity of intervertebral disc cells: phenotype and function. J Anat 2012; 221: 480-496.
[6] An HS, Masuda K, Inoue N. Intervertebral disc degeneration: biological and biomechanical factors. J Orthop Sci 2006; 11: 541-552.
[7] Hiyama A, Skubutyte R, Markova D, Anderson DG, Yadla S, Sakai D, Mochida J, Albert TJ, Shapiro IM, Risbud MV. Hypoxia activates the notch signaling pathway in cells of the intervertebral disc: implications in degenerative disc disease. Arthritis Rheum 2011; 63: 1355-1364.
[8] Johnson ZI, Schoepflin ZR, Choi H, Shapiro IM, Risbud MV. Disc in flames: roles of TNF-alpha and IL-1beta in intervertebral disc degeneration. Eur Cell Mater 2015; 30: 104-116.
[9] Wang H, Tian Y, Wang J, Phillips KL, Binch AL, Dunn S, Cross A, Chiverton N, Zheng Z, Shapiro IM, Le Maitre CL, Risbud MV. Inflammatory cytokines induce NOTCH signaling in nucleus pulposus cells: implications in intervertebral disc degeneration. J Biol Chem 2013; 288: 16761-16774.
[10] Oeckinghaus A, Ghosh S. The NF-kappaB family of transcription factors and its regulation. Cold Spring Harb Perspect Biol 2009; 1: a000034.
[11] Lawrence T. The nuclear factor NF-kappaB pathway in inflammation. Cold Spring Harb Perspect Biol 2009; 1: a001651.
[12] Fang H, Li X, Shen H, Sun B, Teng H, Li P. Osteogenic protein-1 attenuates apoptosis and enhances matrix synthesis of nucleus pulposus cells under high-magnitude compression though inhibiting the p38 MAPK pathway. Biosci Rep 2018; [Epub ahead of print].
[13] Liu G, Cao P, Chen H, Yuan W, Wang J, Tang X. MiR-27a regulates apoptosis in nucleus pulposus cells by targeting PI3K. PLoS One 2013; 8: e75251.
[14] Wang Z, Leng J, Zhao Y, Yu D, Xu F, Song Q, Qu Z, Zhuang X, Liu Y. N-cadherin maintains the healthy biology of nucleus pulposus cells under high-magnitude compression. Cell Physiol Biochem 2017; 43: 2327-2337.
[15] Wapinski O, Chang HY. Long noncoding RNAs and human disease. Trends Cell Biol 2011; 21: 354-361.
[16] DiStefano JK. The emerging role of long noncoding RNAs in human disease. Methods Mol Biol 2018; 1706: 91-110.
[17] Chen X, Yan CC, Zhang X, You ZH. Long noncoding RNAs and complex diseases: from experimental results to computational models. Brief Bioinform 2017; 18: 558-576.
[18] Harries LW. Long non-coding RNAs and human disease. Biochem Soc Trans 2012; 40: 902-906.
[19] Wan ZY, Song F, Sun Z, Chen YF, Zhang WL, Samartzis D, Ma CJ, Che L, Liu X, Ali MA, Wang HQ, Luo ZJ. Aberrantly expressed long noncoding RNAs in human intervertebral disc degeneration: a microarray related study. Arthritis Res Ther 2014; 16: 465.
[20] Zhao B, Lu M, Wang D, Li H, He X. Genome-wide identification of long noncoding RNAs in human intervertebral disc degeneration by RNA sequencing. Biomed Res Int 2016; 2016: 3684875.
[21] Bellelli R, Borel V, Logan C, Svendsen J, Cox DE, Nye E, Metcalfe K, O'Connell SM, Stamp G, Flynn HR, Snijders AP, Lassailly F, Jackson A, Boulton SJ. Polepsilon instability drives replication stress, abnormal development, and tumorigenesis. Mol Cell 2018; 70: 707-721.
[22] Cao J. The functional role of long non-coding RNAs and epigenetics. Biol Proced Online 2014; 16: 11.
[23] Jiang K, Zhang C, Yu B, Chen B, Liu Z, Hou C, Wang F, Shen H, Chen Z. Autophagic degradation of FOXO3a represses the expression of PUMA to block cell apoptosis in cisplatin-resistant osteosarcoma cells. Am J Cancer Res 2017; 7: 1407-1422.
[24] Li Q, Li H, Zhao X, Wang B, Zhang L, Zhang C, Zhang F. DNA methylation mediated downregulation of miR-449c controls osteosarcoma cell cycle progression by directly targeting oncogene c-Myc. Int J Biol Sci 2017; 13: 1038-1050.
[25] Li S. Expression of concern: the functional role of long non-coding RNAs and epigenetics. Biol Proced Online 2016; 18: 12.
[26] Zhang C, Wang B, Zhao X, Li X, Lou Z, Chen X, Zhang F. Iron deficiency accelerates intervertebral disc degeneration through affecting the stability of DNA polymerase epsilon complex. Am J Transl Res 2018; 10: 3430-3442.
[27] Ruan Z, Ma H, Li J, Liu H, Jia H, Li F. The long non-coding RNA NEAT1 contributes to extracellular matrix degradation in degenerative human nucleus pulposus cells. Exp Biol Med (Maywood) 2018; 243: 595-600.
[28] Tang X, Richardson WJ, Fitch RD, Brown CR, Isaacs RE, Chen J. A new non-enzymatic method for isolating human intervertebral disc cells preserves the phenotype of nucleus pulposus cells. Cytotechnology 2014; 66: 979-986.
[29] Wang K, Song Y, Liu W, Wu X, Zhang Y, Li S, Kang L, Tu J, Zhao K, Hua W, Yang C. The noncoding RNA linc-ADAMTS5 cooperates with RREB1 to protect from intervertebral disc degeneration through inhibiting ADAMTS5 expression. Clin Sci (Lond) 2017; 131: 965-979.
[30] Zhang C, Chen B, Jiang K, Lao L, Shen H, Chen Z. Activation of TNF-alpha/NF-kappaB axis enhances CRL4B(DCAF)(11) E3 ligase activity and regulates cell cycle progression in human osteosarcoma cells. Mol Oncol 2018; 12: 476-494.

[31] Zhou Z, Lin Z, Pang X, Tariq MA, Ao X, Li P, Wang J. Epigenetic regulation of long non-coding RNAs in gastric cancer. Oncotarget 2018; 9: 19443-19958.
[32] Zhang C. Essential functions of iron-requiring proteins in DNA replication, repair and cell cycle control. Protein Cell 2014; 5: 750-760.
[33] Zhang C, Zhang F. Iron homeostasis and tumorigenesis: molecular mechanisms and therapeutic opportunities. Protein Cell 2015; 6: 88-100.
[34] Zhou X, Chen L, Grad S, Alini M, Pan H, Yang D, Zhen W, Li Z, Huang S, Peng S. The roles and perspectives of microRNAs as biomarkers for intervertebral disc degeneration. J Tissue Eng Regen Med 2017; 11: 3481-3487.
[35] Zhao B, Yu Q, Li H, Guo X, He X. Characterization of microRNA expression profiles in patients with intervertebral disc degeneration. Int J Mol Med 2014; 33: 43-50.
[36] Qu Z, Quan Z, Zhang Q, Wang Z, Song Q, Zhuang X, Fu C, Xu F, Liu Y, Wang Y, Wang Z, Liu Y. Comprehensive evaluation of differential lncRNA and gene expression in patients with intervertebral disc degeneration. Mol Med Rep 2018; 18: 1504-1512.
[37] Chen Y, Ni H, Zhao Y, Chen K, Li M, Li C, Zhu X, Fu Q. Potential role of lncRNAs in contributing to pathogenesis of intervertebral disc degeneration based on microarray data. Med Sci Monit 2015; 21: 3449-3458.
[38] Moore LD, Le T, Fan G. DNA methylation and its basic function. Neuropsychopharmacology 2013; 38: 23-38.
[39] Jin B, Li Y, Robertson KD. DNA methylation: superior or subordinate in the epigenetic hierarchy? Genes Cancer 2011; 2: 607-617.

Table S1. Basic information of healthy controls (HC) and IDD patients (n=24 in each group)

Parameter	HC	IDD-1	IDD-2	IDD-3	IDD-4	IDD-5
Mean age	45.3±3.2	41.9±3.8	44.6±4.8	46.9±4.1	49.3±3.7	55.3±6.5
Gender	12 M/12 F	12 M/12 F	12 M/12 F	12 M/12 F	12 M/12 F	12 M/12 F
IVD segment	L2-L4	L2-L5	L3-L5	L2-L4	L2-L5	L2-L5

HC, healthy controls; IDD, intervertebral disc degeneration; F, female; M, male.

Table S2. Primers used for qMSP analysis

Gene	Forward Primers	Reverse primers
GAPDH	5'-CGCTTTCTTTCCTTTCGC-3'	5'-TGCCCATTCATTTCCTTCC-3'
Island-1	5'-GTTAAGTGTTGAAGTTTGATGGAGT-3'	5'-TTCATAACCATATCTACATATTCCTTACTA-3'
Island-2	5'-TTGTGTGTTTGTTTTTTTTATTTAGG-3'	5'-CCAACTCAAACATATTCTACTCTATCTAAC3'

Table S3. Differentially expressed lncRNAs in IDD patients compared to healthy control

LncRNA	Average fold change	*P* Value	Expression
ENST00000523452.1	-40.2	0.000054	Down
ENST00000590144.1	-39.4	0.000077	Down
ENST00000549023.1	-38.7	0.00043	Down
ENST00000443565.1	-38.2	0.000051	Down
ENST00000593082.1	-37.4	0.000076	Down
ENST00000558475.1	-36.5	0.000032	Down
ENST00000421891.2	-35.8	0.000012	Down
ENST00000367477.3	-33.6	0.000041	Down
ENST00000447891.1	-33.1	0.000024	Down
ENST00000556200.1	-32.5	0.000016	Down
ENST00000594589.1	-31.9	0.000019	Down
ENST00000589708.1	-30.6	0.000046	Down
ENST00000411690.1	-29.5	0.000025	Down
ENST00000443562.1	-28.9	0.000068	Down
ENST00000437426.1	-28.1	0.000087	Down
ENST00000602530.1	-27.6	0.000054	Down
ENST00000589234.1	-27.2	0.000037	Down
ENST00000445606.1	-26.8	0.000027	Down
ENST00000507856.1	-26.5	0.0000087	Down
ENST00000514793.1	-25.5	0.000092	Down
ENST00000587998.1	-24.8	0.000017	Down
ENST00000415358.1	-24.2	0.000066	Down
ENST00000530313.1	-23.6	0.000037	Down
ENST00000458615.1	-23.4	0.000028	Down
ENST00000558617.1	-22.8	0.000024	Down
ENST00000412132.1	-22.3	0.000037	Down
ENST00000577557.1	-21.8	0.0000063	Down
ENST00000514836.1	-21.5	0.000017	Down
ENST00000485805.1	-21.1	0.000033	Down
ENST00000535936.1	-20.7	0.000084	Down
ENST00000453002.1	-20.3	0.000011	Down
ENST00000511991.1	-19.5	0.000054	Down
ENST00000423802.1	-19.1	0.000058	Down

ENST00000507566.1	-17.9	0.000066	Down
ENST00000440609.1	-16.5	0.000033	Down
ENST00000452932.1	-16.3	0.000028	Down
ENST00000498163.1	-15.2	0.000078	Down
ENST00000408017.1	-14.6	0.000026	Down
ENST00000415172.1	-14.1	0.000073	Down
ENST00000447718.1	-13.2	0.00093	Down
ENST00000411660.1	-12.6	0.000046	Down
ENST00000501280.1	-12.4	0.000051	Down
ENST00000430751.1	-12.1	0.000064	Down
ENST00000401064.1	-11.5	0.000038	Down
ENST00000451959.1	-11.0	0.000026	Down
ENST00000470966.1	-10.4	0.000018	Down
ENST00000472161.1	-9.8	0.000059	Down
ENST00000493002.1	-9.5	0.000074	Down
ENST00000356139.1	-9.2	0.000083	Down
ENST00000440688.1	-8.7	0.000032	Down
ENST00000439324.1	-8.4	0.000021	Down
ENST00000448147.1	-8.1	0.00017	Down
ENST00000498840.1	-7.7	0.000095	Down
ENST00000430431.1	-7.1	0.000035	Down
ENST00000398190.1	-6.6	0.000018	Down
ENST00000499690.1	-6.2	0.000019	Down
ENST00000457248.1	-6.1	0.000038	Down
ENST00000358818.1	-5.7	0.000027	Down
ENST00000423096.1	-5.4	0.000066	Down
ENST00000441522.1	-5.0	0.000043	Down
ENST00000486904.1	-4.3	0.000093	Down
ENST00000501841.1	-3.8	0.00042	Down
ENST00000440936.1	-3.4	0.000053	Down
ENST00000439120.1	-2.5	0.00049	Down
ENST00000520357.1	33.7	0.00083	Up
ENST00000568017.1	32.5	0.00074	Up
ENST00000441379.1	32.1	0.00034	Up
ENST00000588634.1	31.3	0.00065	Up
ENST00000521953.1	30.9	0.000044	Up
ENST00000445483.1	30.5	0.000032	Up
ENST00000428911.1	29.9	0.000043	Up
ENST00000437751.1	29.4	0.000077	Up
ENST00000428573.1	29.1	0.000022	Up
ENST00000540987.1	28.4	0.00099	Up
ENST00000579378.1	27.7	0.000021	Up
ENST00000501897.1	27.2	0.000053	Up
ENST00000499096.2	26.4	0.000052	Up
ENST00000527514.1	26.1	0.000099	Up
ENST00000577684.1	25.6	0.00016	Up
ENST00000500944.2	25.1	0.000043	Up
ENST00000464242.1	24.6	0.000088	Up
ENST00000426709.1	24.2	0.000082	Up

ENST00000471672.1	23.8	0.000031	Up
ENST00000522057.1	23.4	0.000052	Up
ENST00000506196.1	22.8	0.00054	Up
ENST00000443579.1	22.4	0.00046	Up
ENST00000442146.1	22.1	0.000032	Up
ENST00000433012.1	21.5	0.00019	Up
ENST00000431362.1	21.2	0.00011	Up
ENST00000453100.1	20.6	0.000054	Up
ENST00000544414.1	20.2	0.000032	Up
ENST00000533528.1	19.6	0.00047	Up
ENST00000558831.1	19.4	0.000078	Up
ENST00000456450.1	18.7	0.00055	Up
ENST00000455216.1	18.3	0.000012	Up
ENST00000405359.1	17.4	0.000054	Up
ENST00000398740.1	16.7	0.000033	Up
ENST00000396351.1	15.2	0.000099	Up
ENST00000506795.1	14.5	0.000012	Up
ENST00000428356.1	13.7	0.00035	Up
ENST00000377305.1	13.2	0.00076	Up
ENST00000421380.1	12.5	0.00014	Up
ENST00000443888.1	11.3	0.00066	Up
ENST00000512502.1	10.9	0.00054	Up
ENST00000490423.1	10.2	0.00032	Up
ENST00000473923.1	9.6	0.00081	Up
ENST00000499139.1	8.8	0.00017	Up
ENST00000441356.1	8.0	0.00066	Up
ENST00000445125.1	7.3	0.00042	Up
ENST00000400311.1	6.6	0.00077	Up
ENST00000446309.1	6.2	0.00074	Up
ENST00000441087.1	5.4	0.000043	Up
ENST00000411825.1	4.8	0.00017	Up
ENST00000451291.1	4.2	0.00012	Up
ENST00000514487.1	3.4	0.00063	Up
ENST00000423637.1	3.2	0.00032	Up
ENST00000429536.1	2.7	0.00098	Up
ENST00000450217.1	2.4	0.00014	Up
ENST00000439477.1	2.1	0.00011	Up